Available online at www.sciencedirect.com
SCIENCE DIRECT®

Polymer 44 (2003) 4723–4734

polymer

www.elsevier.com/locate/polymer

# Crystallization kinetics and morphological behavior of reactively processed PBT/epoxy blends

Bhawna Kulshreshtha, Anup K. Ghosh, Ashok Misra*

*Centre for Polymer Science and Engineering, Indian Institute of Technology, Delhi, Hauz Khas New Delhi 110 016, India*

Received 20 August 2002; received in revised form 10 March 2003; accepted 15 April 2003

**Abstract**

Polybutylene terephthalate (PBT), a versatile engineering thermoplastic, has been processed using epoxy resin as a reactive solvent. Following processing of this blend, the epoxy was cured using a bi-functional amine curing agent, resulting in phase separation and phase inversion thus producing a different morphology. Change in crystallization kinetics of PBT in the presence of the epoxy monomer and cured epoxy resin has been studied using differential scanning calorimetry. Half time of crystallization ($t_{1/2}$) of PBT decreased in the presence of epoxy monomer while it remained constant in the presence of cured epoxy resin. The value of Avrami exponent varied between 1 and 2 in pure PBT as well as for uncured and cured blends, indicating mixed type of spherulitic growth. Morphology of the uncured and cured blends was studied using small angle light scattering (SALS) and polarizing microscopy for samples crystallized at different temperatures at all levels of the epoxy resin. Scattering pattern in $H_v$ and $V_v$ mode of SALS provided information about the type of spherulites as well as volume filling nature of the spherulites. In general, typical unusual type of spherulitic pattern for PBT, in which scattering lobes lie along the polar axis, changed to usual type of pattern for PBT/epoxy blends, in which scattering lobes lie at 45° to the polar axis.

*Keywords:* Polybutylene terephthalate; Crystallization kinetics; Epoxy resin

## 1. Introduction

Polybutylene terephthalate (PBT) is a semi-crystalline polymer with high commercial value and due to its good chemical resistance, high melting temperature and good dimensional stability, it is a material of major interest for numerous applications. Although PBT can be relatively easily processed, a further improvement of processability is required in order to obtain an increased adaptability to specific processing requirements, e.g. flow length or mould geometry. The processing characteristics of polymers can be improved by using solvents. Disadvantage of using solvent is that it involves a tedious and time consuming step of solvent removal. Besides this the solvent can be hazardous to environment also. Venderbosch et al. [1–4] used epoxy resin as reactive solvent to lower the processing temperature of poly(2,6-dimethyl-1,4-phenylene ether) (PPE). In this route, the polymer to be processed is dissolved in a monomer (reactive solvent) and a homogeneous solution is obtained. The homogeneous solution is then transferred into a mold. Upon polymerisation in the mold, as the molecular weight of the reactive solvent (monomer) increases, phase separation and phase inversion take place so that dissolved polymer becomes the continuous matrix and reactive solvent is obtained in the form of dispersed phase in the thermoplastic matrix. Final properties of the system are generally dominated by the thermoplastic phase. The main advantage of this route is that both processing temperature and viscosity are lowered. Furthermore, there is no need for the removal of the solvent.

The same processing route of using epoxy resin as reactive solvent has been explored for the processing of PBT with a view to improve the processing characteristics of PBT. The schematic outline of this route has been shown in Fig. 1. Furthermore, PBT has been blended with several thermoplastics to modify its properties, however, relatively little attention has been given on its blends with thermosets. Therefore this study provides detailed information on the

---

* Corresponding author. Present address. India Institute of Technology, Mumbai, Powai, 400 076, India.

*E-mail address:* amisra@iitb.ac.in (A. Misra).

0032-3861/03/$ - see front matter © 2003 Elsevier Science Ltd. All rights reserved.
doi:10.1016/S0032-3861(03)00347-1

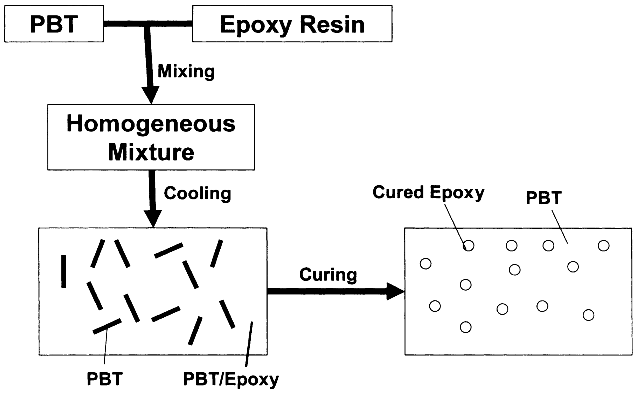

Fig. 1. Schematic representation of the processing technique using reactive solvent.

blends of PBT with epoxy resin. This reactive processing route has been reported to be used for the processing of several thermoplastics, e.g. high density polyethylene (HDPE), poly(methylmethacrylate) (PMMA), polystyrene (PS) and poly(ethyleneterephthalate) (PET) [5–9].

In the polymer blends, where one component is crystalline and the another one is amorphous, the curing of second component results in chain extension, branching, cross-linking and significant changes in chemical and physical properties of the non-crystalline component. Hence an investigation of crystalline perfection and morphology of crystalline component becomes very important in these type of systems. PBT shows two types of spherulites, usual and unusual type. In the usual type, the optic axis is along the spherulitic radius radial direction while in the unusual type, the optic axis is at an angle of 45° to the spherulitic radius. Ludwig and Eyerer [10] reported that melt enthalpy of the usual spherulites is larger than the melt enthalpy of the unusual type (60 J/g for the usual type and 48 J/g for the unusual type). Spherulitic morphology of PBT was studied using small angle light scattering (SALS) in $H_v$ and $V_v$ modes by Stein et al. [11,12]. Misra and Stein [12] have reported that PBT shows unusual spherulites for crystallization temperature between 0 and 180 °C and usual spherulites at 200 °C. Roche et al. [13] reported that in the case of PBT, the formation of unusual type of spherulites is the fundamental structural feature. Misra and Garg [14–16] have reported the change in spherulitic pattern of PBT in the presence of PET and change in the spherulitic pattern of PET in the presence of a polyamide. Unusual pattern of PBT changes into usual pattern in PBT–PC blends as PC content is increased above 30 wt% [17].

In the present work, PBT was blended with epoxy resin to enhance its processing characteristics and adaptability for specific requirements. Effect of uncrosslinked and crosslinked epoxy resin on the rate of crystallization and spherulitic morphology has been presented in this paper.

## 2. Experimental

### 2.1. Materials and blend preparation

The materials used are polybutylene terephthalate (PBT), Valox 315 ($M_w = 115{,}000$ g/mol) from GE Plastics, Netherlands; epoxy resin, Epikote 828 (diglycidyl ether of bisphenol-A), supplied by Shell, Netherlands. A bi-functional amine curing agent, 4,4′-methylene bis(3-chloro-2, 6 diethyl aniline) (M-CDEA), supplied by Lonza Chemicals, Netherlands was used for the curing of epoxy resin.

PBT powder was dried at 80 °C for 24 h. PBT and epoxy resin blends (in the absence of curing agent) with an epoxy content of 10–50 wt% were prepared in a miniature co-rotating twin-screw extruder (6 $\text{cm}^3$ volume) at 220 °C and 150 rpm. Extruded strands were pelletized and ground into fine particles.

PBT/epoxy resin blends with stoichiometric amount of curing agent with an epoxy content of 10–50 wt% were prepared in a Brabender Plasticorder Kneader (with a volume of 300 $\text{cm}^3$) at 220 °C and 50 rpm. A kneading time of around 45 min was required to obtain transparent homogeneous solutions. The curing agent was added to the homogeneous solution in the Brabender Kneader and after mixing for 8–10 min, the mixture was compression moulded and cured for 4 h at 175 °C.

### 2.2. Differential scanning calorimetry (DSC)

A Perkin–Elmer Pyris differential scanning calorimeter (DSC7) was used to detect the heat flow from the samples during isothermal crystallization from the melt. All the measurements were conducted under nitrogen atmosphere and calibrated using an Indium standard. To determine the optimum concentration of curing agent, blends of PBT with 30 wt% epoxy resin and different percentage of curing agent (45–60 parts per hundred parts of resin by weight (phr)) were prepared in mini-mixer and their melting endotherms were recorded by heating the sample from 50 to 250 °C at a rate of 10 °C/min.

For isothermal crystallization studies, all the samples were first heated up to 250 °C and were kept at this temperature for 3 min in order to remove any thermal history. They were then quenched to a predetermined crystallization temperature ($T_c$) at a rate of 300 °C/min. The samples were kept at this temperature for 15 min and relative degree of crystallinity, $X_t$ was determined from the heat generated during the development of the crystalline phase as follows:

$$X_t = \frac{\int_{t_0}^{t} \left(\frac{dH}{dt}\right) dt}{\int_{t_0}^{\infty} \left(\frac{dH}{dt}\right) dt} \tag{1}$$

where $t_0$ is the time at which the sample attains isothermal condition, numerator is the heat generated at time $t$ and the denominator is the total heat generated for the complete crystallization.

### 2.3. Small angle light scattering

The spherulitic morphology of the blend was observed using SALS technique. The samples were examined using photographic SALS apparatus attached to a 10 MW He–Ne source. Photographs of the SALS pattern were recorded using CCD camera which were then analysed using Leica Qwin software. The spherulite size was calculated using the following relation [18]:

$$R = 1.025\lambda_0/\pi n \sin(\theta'_{\rm m}/2) \tag{2}$$

where, $R$ is the average spherulitic radius, $\lambda_0$ is the wavelength of light in air, $n$ is the refractive index of the sample, and $\theta'_{\rm m}$ is the corrected scattering angle for maximum intensity, which is related to the actual scattering angle, $\theta_{\rm m}$ as,

$$\sin\theta'_{\rm m} = \sin\theta_{\rm m}/n \tag{3}$$

PBT/epoxy uncured and cured blends with epoxy amount varying from 10 to 50 wt% were melted at 250 °C and then transferred at 50 °C. The samples were crystallized for 5 min and quenched in ice-cold water. Change in the type of superstructure with increasing amount of epoxy resin was recorded and analysed.

For SALS studies, samples in the form of fine particles were pressed between two glass slides and heated at a rate of 10 °C/min to the molten state and subsequently quenched at a crystallization temperature varying between 50 and 215 °C. The samples were then crystallized at these temperatures for 5 min and quenched rapidly in ice–water mixture. The formation of type of superstructure was recorded and analysed.

## 3. Results and discussion

The optimum concentration of curing agent for the epoxy in PBT/epoxy blends was determined using DSC by following the melting point at different levels of the curing agent. For this PBT/epoxy 70/30 blend was used in which the curing agent concentration was varied from 45 to 60 phr. All the blends were cured for 4 h at 175 °C. It is reported that M-CDEA is compatible with PBT [19], hence instead of using stoichiometric amount of curing agent, some excess amount of curing agent is required in order to compensate for any loss of M-CDEA due to dissolution in the PBT phase. The concentration of curing agent that would result in highest melting temperature of the PBT/epoxy cured blends has been considered as optimal curing agent concentration since no epoxy is available for depression in melting point. The melting temperature of the cured blends determined using DSC are shown in Fig. 2, as a function of concentration of curing agent. In a similar study, Oyanguren et al. [19,20] have reported the conversion-temperature transformation diagram (CTT) for a PBT/DGEBA/M-CDEA system containing 3.3 and 6.6 wt.% of PBT and have reported increase in the melting temperature, $T_{\rm m}$, with the conversion reaching the value of pure PBT at full conversion. Highest melting point of PBT is reached at highest cross-link density of epoxy phase. It is, however, remarkable that optimum value for the curing agent concentration coincides with the stoichiometric concentration for the neat epoxy resin/M-CDEA system (50 part per hundred parts of resin by weight) in the present study.

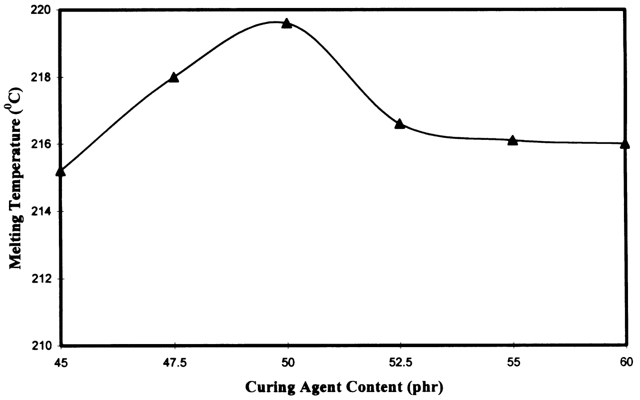

Fig. 2. Variation of melting temperature with increasing M-CDEA concentration in 70/30 PBT/epoxy blend cured at 175 °C for 4 h.

Crystallization isotherms obtained by plotting reduced crystallinity, $X_{\rm t}$ with respect to time $t$ are shown in Figs. 3 and 4 for PBT and PBT/epoxy uncured and cured blends, respectively. The crystallization isotherms are sigmoidal in shape. The half time of crystallization, $t_{1/2}$, defined as the

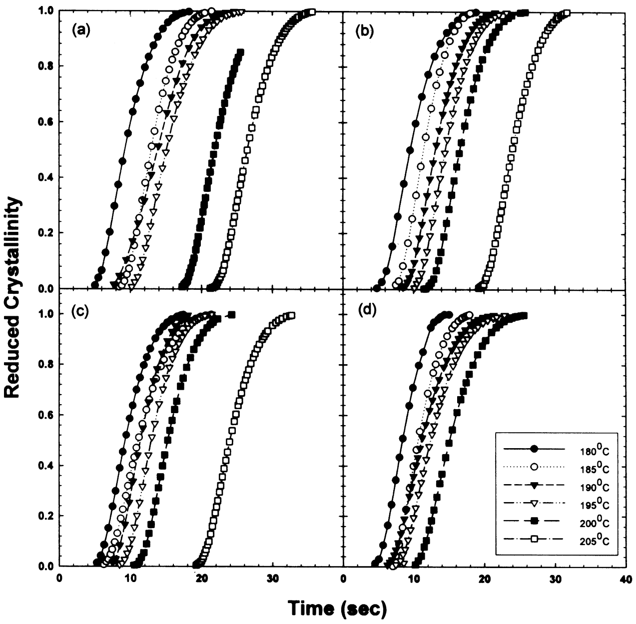

Fig. 3. Plots of reduced crystallinity vs. time for uncured PBT/epoxy blends; (a) PBT (b) 90/10 (c) 80/20 and (d) 70/30.

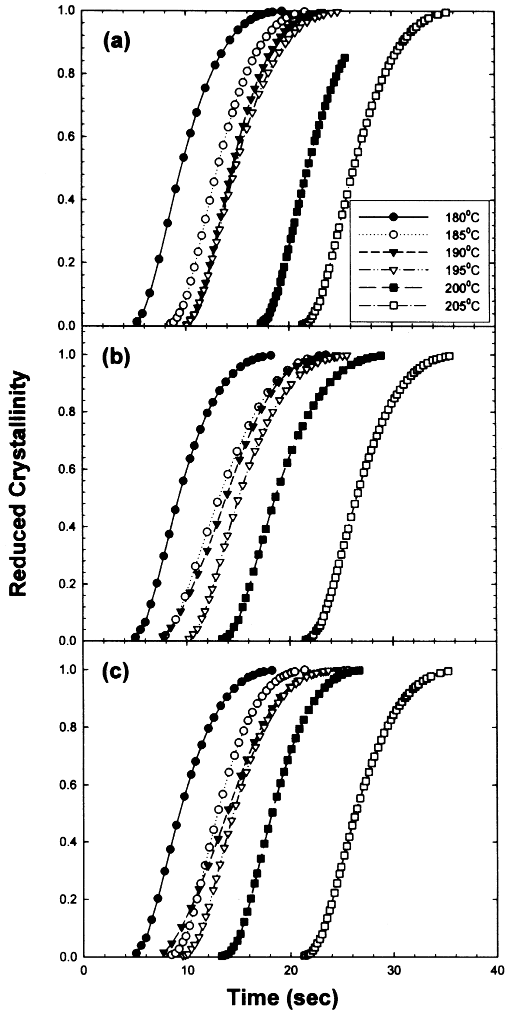

Fig. 4. Plots of reduced crystallinity vs. time for cured PBT/epoxy resin blends; (a) 90/10 (b) 80/20 and (c) 70/30.

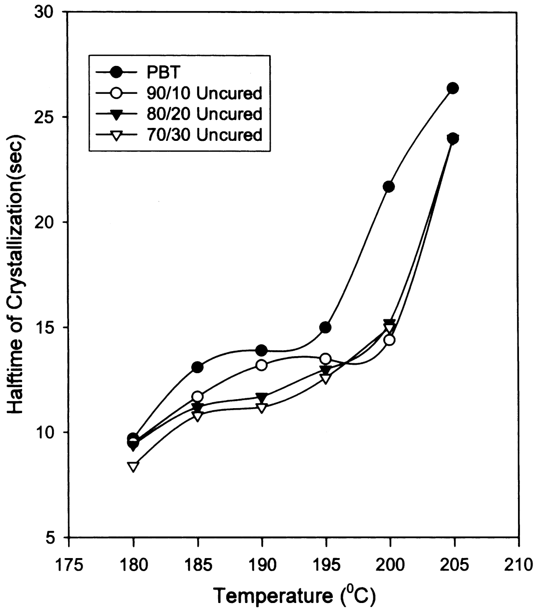

Fig. 5. Variation in half time of crystallization with crystallization temperature for PBT and PBT/epoxy uncured blends.

time required for the development of the half of the final crystallinity was evaluated from these curves and are listed in Table 1 and plotted in Figs. 5 and 6. For pure PBT as well as uncured and cured blends, half time of crystallization goes on increasing with the increasing crystallization temperature. It can be observed that the incorporation of epoxy resin into PBT decreases the $t_{1/2}$ and increases the overall crystallization rate of PBT at all temperatures. The kinetics of isothermal crystallization from the melt of uncured and cured blends was analysed on the basis of Avrami equation [21,22]:

$$\log[-\ln(1 - X_t/X_\infty)] = n \log t + \log K \tag{4}$$

where $K$ is the crystallization rate constant associated with the rate of nucleation and $n$ is the Avrami exponent, the value of which depends on the primary nucleation and growth geometry of the crystalline entities. $X_t$ is the crystallinity developed after time $t$ and $X_\infty$ is the crystallinity developed after infinite time period.

Figs. 7 and 8 present the plot of $\log[-\ln(1 - X_t/X_\infty)]$ with respect to $\log t$ for PBT/epoxy uncured and cured blends, respectively. The experimental data are fitted by the Avrami equation only for the early part of transformation. For many systems, Avrami equation is found to be valid only at low conversions [23]. Therefore, the experimental data at low conversion regions was used to evaluate $K$ and $n$.

Table 1
Values of Avrami exponent ($n$) and rate constant ($K$) at various crystallization temperatures for PBT/epoxy uncured and cured blends

| Blend composition PBT/epoxy | $T_c$ = 180 °C[a] | | $T_c$ = 185 °C | | $T_c$ = 190 °C | | $T_c$ = 195 °C | | $T_c$ = 200 °C | | $T_c$ = 205 °C | |
|---|---|---|---|---|---|---|---|---|---|---|---|---|
| | $n$ | $K \times 10^{-3}$ | n | $K \times 10^{-3}$ | $n$ | $K \times 10^{-3}$ | $n$ | $K \times 10^{-3}$ | $n$ | $K \times 10^{-3}$ | $n$ | $K \times 10^{-3}$ |
| 100/0 | 2.0 | 7.9 | 1.7 | 4.8 | 2.2 | 8.4 | 1.9 | 1.5 | 1.5 | 5.6 | 1.6 | 1.6 |
| 90/10 (uncured) | 2.8 | 2.1 | 2.3 | 6.8 | 1.8 | 4.0 | 1.9 | 1.0 | 1.9 | 1.2 | 1.3 | 4.0 |
| 80/20 (uncured) | 2.2 | 7.4 | 1.8 | 4.7 | 1.7 | 4.9 | 1.7 | 4.8 | 2.0 | 6.3 | 1.5 | 3.2 |
| 70/30 (uncured) | 2.2 | 6.7 | 1.8 | 2.6 | 1.8 | 4.6 | 1.6 | 5.6 | 1.9 | 1.5 | – | – |
| 90/10(cured) | 2.3 | 6.8 | 1.9 | 4.0 | 1.9 | 1.2 | 2.7 | 2.3 | 2.1 | 3.4 | 1.5 | 2.5 |
| 80/20(cured) | 2.0 | 7.7 | 1.7 | 3.6 | 2.2 | 8.4 | 1.9 | 1.5 | 1.8 | 4.0 | 1.6 | 5.1 |
| 70/30(cured) | 2.0 | 7.5 | 1.6 | 2.5 | 2.3 | 5.0 | 1.8 | 6.8 | 1.6 | 2.2 | 1.6 | 2.5 |

[a] $T_c$ = temperature of crystallization.

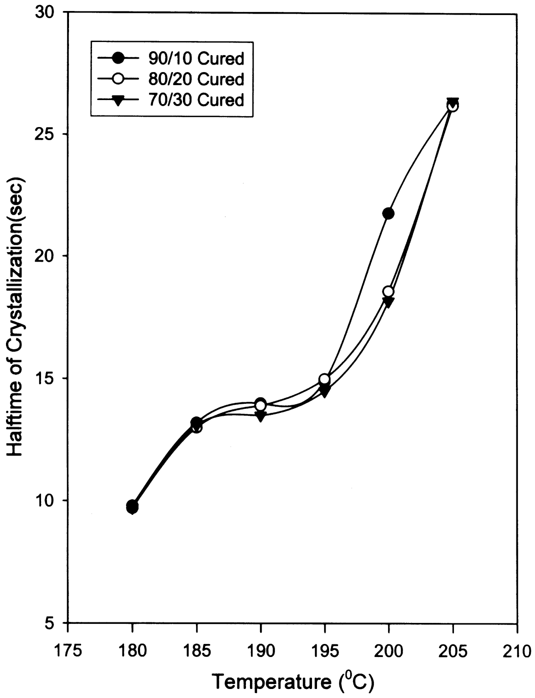

Fig. 6. Variation in half time of crystallization with crystallization temperature for PBT/epoxy cured blends.

The values of $K$ and $n$ were determined by the intercept and slope, respectively, of the straight line and are listed in Table 1. The values of $n$ are found to be between 1 and 2 for PBT as well as for the blends studied, which indicate the contribution of different growth processes for the PBT and PBT/epoxy blends. Pure PBT shows mostly polyhedral (spherulitic) growth. The observed value of $n$ for PBT (between 1 and 2) is lower than the theoretically predicted Avrami exponent value of 3 for spherulitic growth with heterogeneous nucleation. This can be attributed to a high nucleation density and truncation of spherulites. The growth geometry for the blends, on the other hand, is mostly two-dimensional (platelike or disclike), assuming the possibility of a large number of nucleation. The $n$ values observed in the case of pure PBT as well as uncured and cured blends are found to be in the same range and no change was observed with incorporation of the epoxy resin.

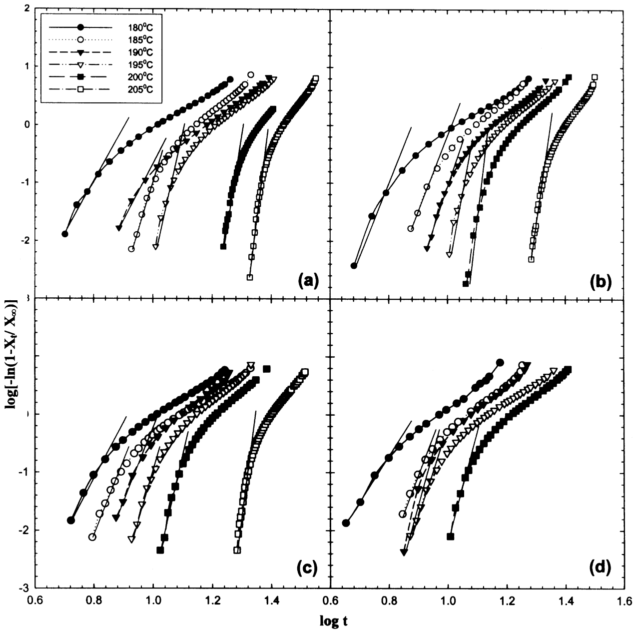

Fig. 7. Avrami plots of $\log[-\ln(1 - X_t)]$ vs. $\log t$ for uncured PBT/epoxy uncured blends; (a) PBT (b) 90/10 (c) 80/20 and (d) 70/30.

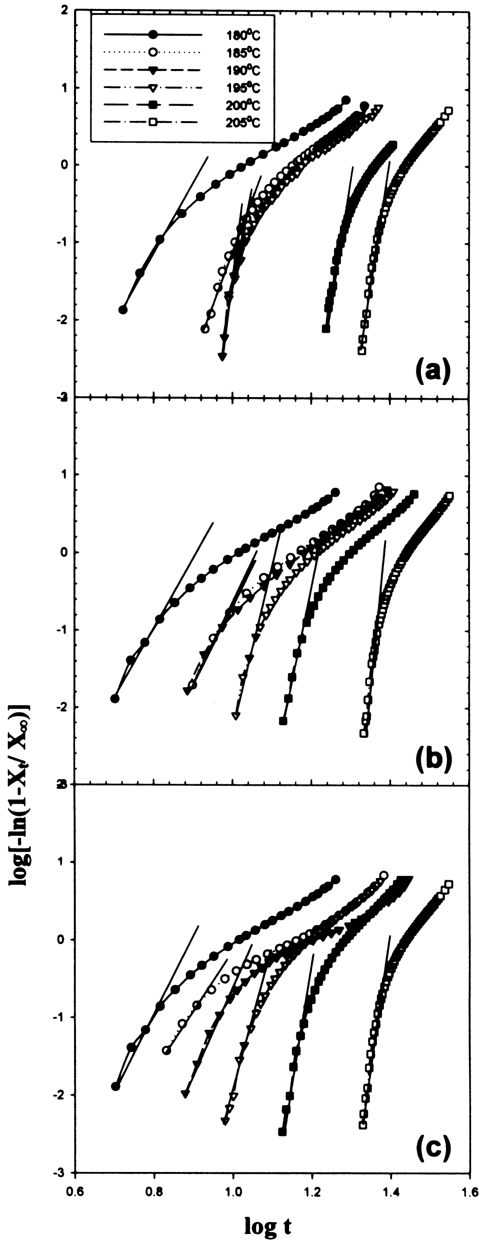

Fig. 8. Avrami plots of $\log[-\ln(1 - X_t)]$ vs. $\log t$ for PBT/epoxy cured blends; (a) 90/10 (b) 80/20 and (c) 70/30.

Figs. 9 and 10 show a series of $H_v$ SALS pattern and corresponding optical micrograph for PBT and PBT/epoxy uncured and cured blends, respectively, isothermally crystallized at 50 °C. Pure PBT shows four lobe unusual

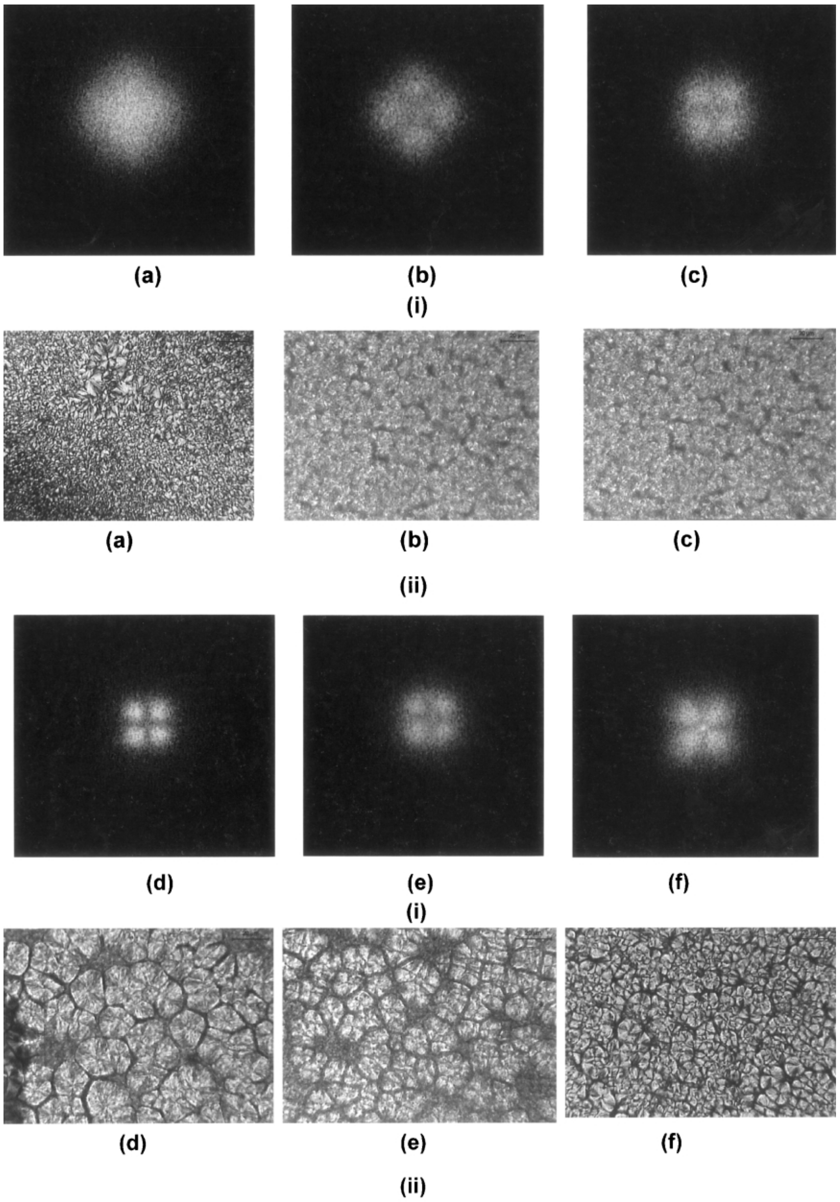

Fig. 9. (i) SALS $H_v$ patterns and (ii) corresponding optical micrographs for PBT/epoxy uncured blends crystallized at 50 °C; (a) PBT (b) 90/10 (c) 80/20 (d) 70/30 (e) 60/40 and (f) 50/50.

type of pattern as has been reported earlier [12]. In both uncured and cured systems, PBT/epoxy 90/10 blend continues to show unusual type of $H_v$ scattering pattern while the pattern changed into four lobe usual type in all blends with 20% or greater amount of epoxy resin. Average spherulitic radius was determined using Eq. (2) and has been plotted with increasing amount of epoxy resin in Fig. 11 for uncured as well as cured system. In the uncured blends, the radius of spherulites increases up to 30% epoxy resin, after which radius starts decreasing. Maximum radius is observed with 30% epoxy resin. The reason may be that up to 30% epoxy resin, size of spherulites is mainly governed by the growth of the spherulites. As epoxy amount increases, spherulites find enough space to grow with less truncation due to dilution effect and hence an increase in the radius is observed. Increase in the onset of nucleation and rate of crystallization was also observed with the increase in epoxy content as reported earlier [24]. As epoxy amount is increased further, there is no hindrance in the growth because of reduced truncation or interference effect, therefore beyond 30% epoxy resin, nucleation becomes the governing factor and as a result, decrease in spherulite radius is observed. In the cured blends, radius increases up to 20% epoxy resin, after which it becomes constant. The increase up to 20% epoxy may be because of dilution effect of cured epoxy resin. Radius is mainly governed by the growth of spherulites up to 20% epoxy resin. In the cured blends, rate of nucleation remains constant with increasing amount of epoxy resin, hence radius of spherulites do not show any appreciable change. In the case of cured blends,

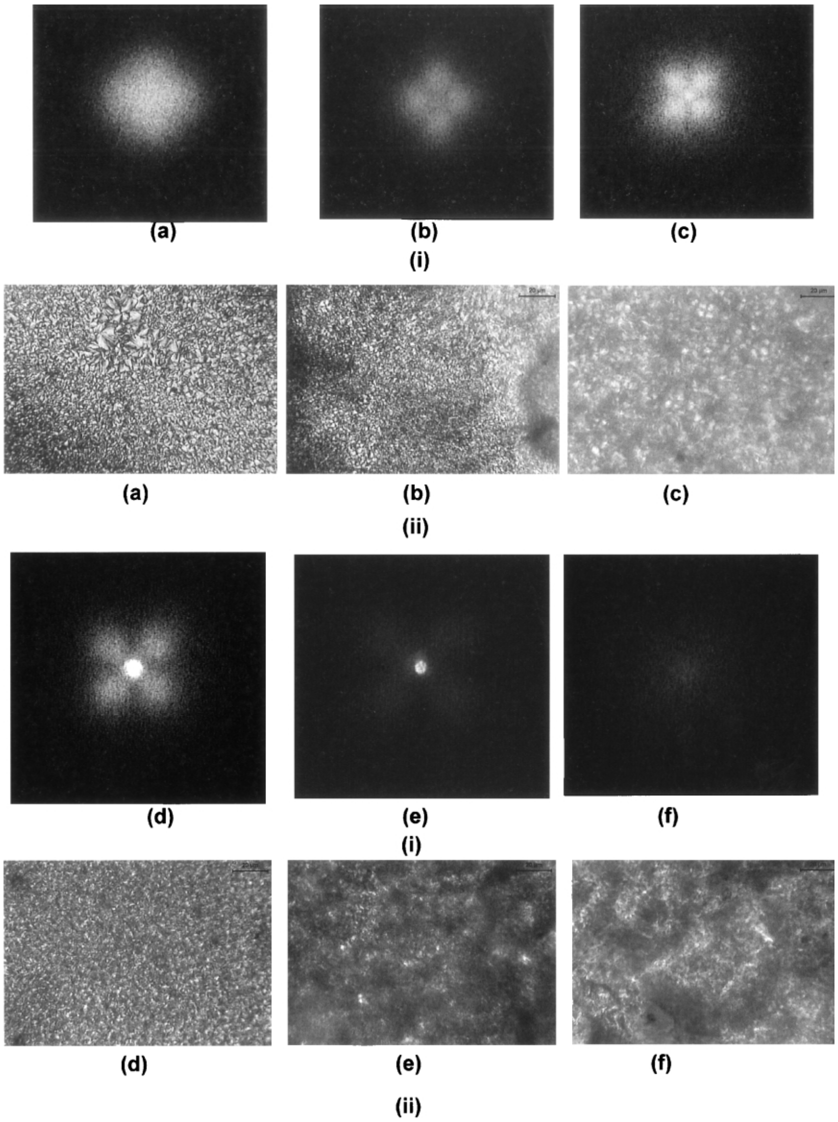

Fig. 10. (i) SALS $H_v$ patterns and (ii) corresponding optical micrographs for PBT/epoxy cured blends crystallized at 50 °C; (a) PBT (b) 90/10 (c) 80/20 (d) 70/30 (e) 60/40 and (f) 50/50.

with 40 and 50% epoxy resin, the intensity of pattern in $H_v$ mode diminishes because of the presence of glassy epoxy resin and hence the radius of spherulites could not be determined. Examination of the crystallized PBT/epoxy uncured blends under a polarizing microscope (PM) showed an increase in the radius up to 30% epoxy resin. Beyond 30% epoxy resin, radius starts decreasing, thus supporting the SALS observations. In the cured blends, superstructure was not readily identifiable because of the presence of glassy epoxy resin.

A series of SALS $V_v$ patterns for PBT and PBT/epoxy uncured blends isothermally crystallized at 50 °C are presented in Fig. 12. Pure PBT shows four lobes at 45° with respect to polar axis, typical of unusual type of spherulites. The four lobe symmetry is changed into the circular symmetry in the presence of 10–20% epoxy resin. The pattern takes two fold symmetry in the presence of 30% and greater epoxy resin.

Intensities of $V_v$ patterns were compared with the corresponding $H_v$ patterns from $I$ vs. $\theta$ plots and the ratio of $I(V_v)/I(H_v)$ values are given in Table 2 for pure PBT and all the blends. In pure PBT, the intensity of $V_v$ pattern was found to be comparable with that of the $H_v$ pattern, thus indicating the formation of volume filled spherulites. In the presence of 10% or greater epoxy resin, the intensity of $V_v$ pattern is high as compared to the intensity of $H_v$ pattern. Hence in the presence of epoxy resin, non-volume filled spherulites are formed. This was confirmed by examining the samples under a PM (Figs. 9 and 10). The composition of the spherulitic and non-spherulitic region was examined from the photomicrographs using Leica Qwin image analyzer which gives the area on the basis of colour

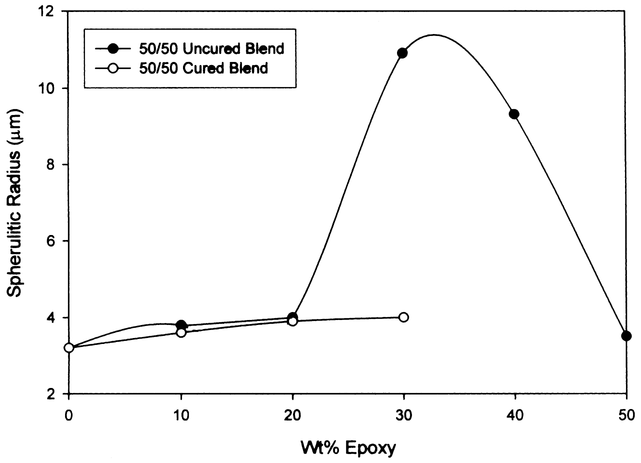

Fig. 11. Plot of spherulitic radius for PBT/epoxy uncured and cured blends isothermally crystallized at 50 °C vs. amount of epoxy resin.

selection and is given in Table 3. In the uncured blends the volume fraction of spherulitic region is greater compared to the actual amount of PBT, the crystallisable component. This indicates that a part of amorphous epoxy is included in the spherulite. It is further seen that the crystallinity of the spherulite (normalized crystallinity of PBT) is greater than that of pure PBT. This suggests that the presence of epoxy enhances the crystallinity of PBT, as has been reported in our earlier paper [24]. Small angle X-ray studies show an increase in the long period and the amorphous thickness, which supports the suggestion that the epoxy is present in the interlamellar region, i.e. within the spherulites, resulting in an increase in the spherulitic region (Table 4). The details of the SAXS studies are presented elsewhere [25]. On the other hand, in the cured blends the volume fraction of the spherulitic region is less as compared to the actual amount of PBT. Along side, the spherulitic crystallinity is also lower than that of pure PBT. This is due to the fact that after curing, epoxy phase separates out and is not part of spherulites as in the uncured case. The network formed by the epoxy also hinders crystallization of PBT thus lowering the crystallinity [24]. SAXS studies further confirm this as there is a decrease in the long period, crystalline as well as amorphous thickness, as seen from the limited data of 90/10 blend [25].

SALS pattern in the $H_v$ mode and the $V_v$ mode for PBT and PBT/epoxy 80/20 uncured and cured blends isothermally crystallized at temperatures of 75, 125 and 200 °C are presented in Figs. 13–15, respectively. SALS patterns at other temperatures (150 and 175 °C) follow trends similar to that of 125 °C and thus have not been shown. Morphological parameters determined from this study are presented in Table 5. At 75 °C, pure PBT gives four lobe unusual type $H_v$ pattern, in which scattering lobes are parallel to the polar axes while PBT/epoxy 80/20 uncured and cured blends show four lobe usual type $H_v$ pattern in which scattering lobes are at 45° to the axis of polarizers. In the $V_v$ mode, pure PBT shows unusual type four lobe pattern in which the scattering lobes are at 45° to the axis of polarizers. The unusual type of pattern changed to usual type of pattern with two major lobes along the polarizer and two minor lobes along the analyzer direction in the presence of 20% epoxy resin in both uncured and cured blends. In the $V_v$ mode, maximum intensity is found to be located at the centre which decreases monotonically towards the corners of the lobes. In pure PBT, the pattern always remained of the unusual type with an increase in the crystallization temperature, however, the size of the pattern decreased, indicating an increase in the spherulitic radius. The increase in the radius of spherulites levels off at 200 °C. The pattern becomes somewhat diffused with increase in the crystallization temperature, which may be due to secondary crystallization. The spherulitic nature of the SALS patterns was confirmed by polarizing microscopic operations.

In the PBT/epoxy 80/20 uncured blend, four lobe usual type pattern changed to the mixed type pattern at $T_c$ of 125 °C. This may be because of the presence of both usual and unusual type of spherulites. The pattern remained the same up to 175 °C with increase in the spherulitic radius. The increase in the radius of spherulites levels off at 175 °C. However, the pattern changed to the unusual type at 200 °C. In the PBT/epoxy 80/20 cured blends, with increase in the crystallization temperature, the pattern always remained of

Table 2
$I_{V_v}/I_{H_v}$ values for PBT in uncured and cured blends, isothermally crystallized at 50 °C

| Blend composition (PBT/epoxy) | $I_{V_v}/I_{H_v}$ (uncured blends) | $I_{V_v}/I_{H_v}$ (cured blends) |
|---|---|---|
| 100/0 | 1.0 | 1.0 |
| 90/10 | 1.2 | 1.4 |
| 80/20 | 1.3 | 1.8 |
| 70/30 | 1.6 | 2.0 |
| 60/40 | 1.6 | – |
| 50/50 | 1.6 | – |

Table 3
Analysis of volume occupied by spherulites and their crystallinity for uncured and cured blends isothermally crystallized at 50 °C

| Blend composition (PBT/epoxy) | Spherulitic region (%) | Nonspherulitic region (%) | Normalized crystallinity (%) |
|---|---|---|---|
| 100/0 | 100 | – | 30.0 |
| 90/10(uncured) | 97.4 | 2.6 | 32.3 |
| 80/20(uncured) | 88.0 | 12.0 | 36.3 |
| 70/30(uncured) | 79.0 | 21.0 | 38.4 |
| 60/40(uncured) | 73.0 | 27.0 | 42.8 |
| 50/50(uncured) | 68.0 | 32.0 | 44.8 |
| 90/10(cured) | 81.0 | 19.0 | 25.8 |
| 80/20(cured) | 64.0 | 36.0 | 19.8 |
| 70/30(cured) | 52.0 | 48.0 | 19.2 |
| 60/40(cured) | 35.0 | 65.0 | 15.4 |
| 50/50(cured) | 30.0 | 70.0 | 13.4 |

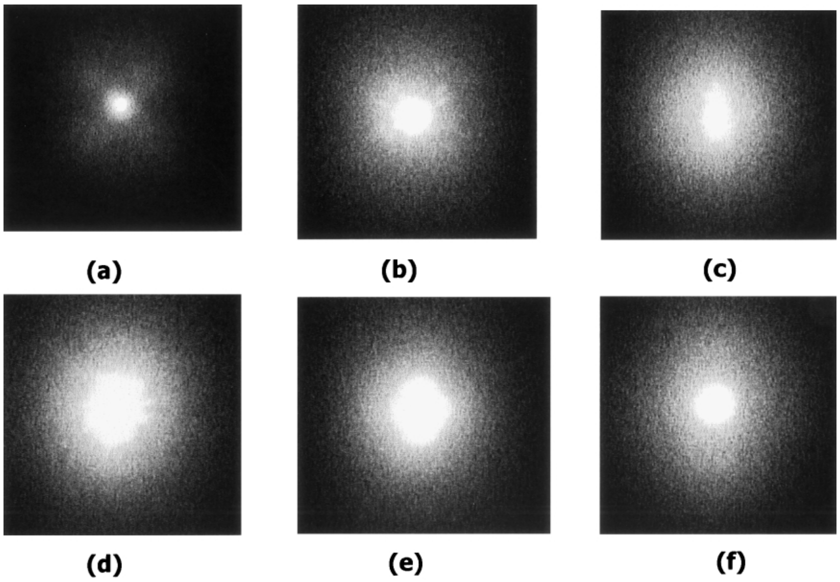

Fig. 12. SALS $V_v$ patterns for PBT/epoxy uncured blends crystallized at 50 °C; (a) PBT (b) 90/10 (c) 80/20 (d) 70/30 (e) 60/40 and (f) 50/50.

the usual type with increase in the spherulitic radius. The increase in the radius levels off at 175 °C.

In pure PBT as well as PBT/epoxy 80/20 uncured and cured blends, an increase in the spherulitic radius is observed with increase in the crystallization temperature (Fig. 16). This indicates a lower nucleation rate at high temperature of crystallization. Intensities of $V_v$ patterns were compared with the corresponding $H_v$ patterns from $I$ vs. $\theta$ plots and $I(V_v)/I(H_v)$ values obtained were calculated for pure PBT and all the blends at temperature between 50 and 215 °C. The values are shown in Table 5. It is known that $V_v$ scattering arises from both density fluctuations as well as anisotropy, whereas $H_v$ scattering arises only from anisotropy [26]. In pure PBT, $V_v$ intensity is found to be comparable to that of $H_v$ intensity which indicates that the spherulitic superstructure is volume filling in the PBT. The higher $V_v$ intensity in all the blends suggests that the spherulitic superstructure is non-volume-filling in the presence of the epoxy.

## 4. Conclusion

Processing of PBT employing a novel technique by

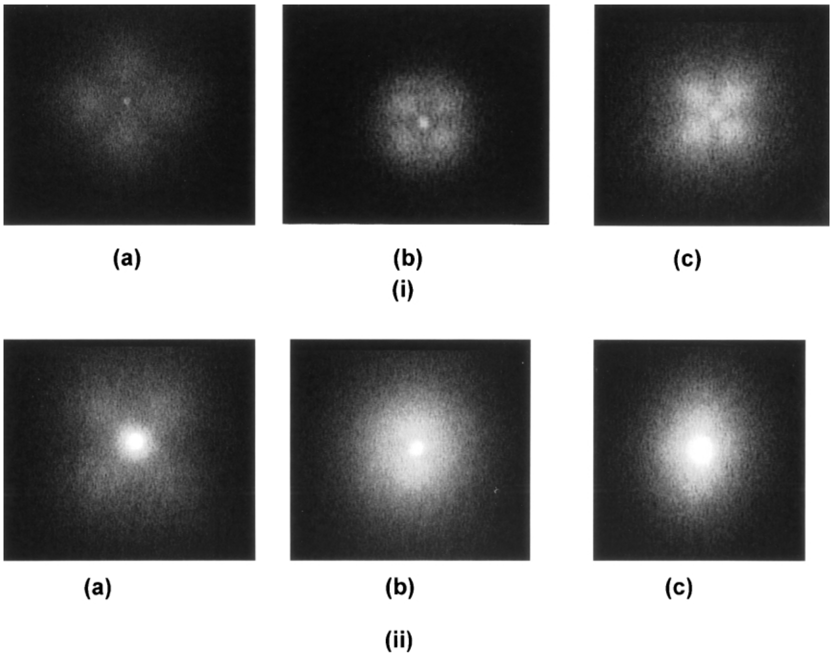

Fig. 13. (i) $H_v$ and (ii)$V_v$ SALS patterns for PBT/epoxy blends crystallized at 75 °C; (a) PBT (b) 80/20 uncured blend (c) 80/20 cured blend.

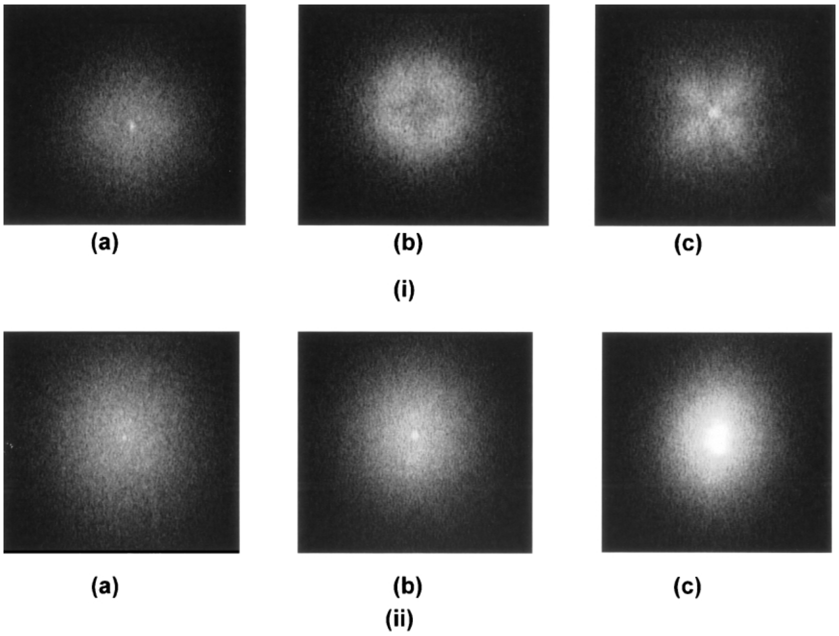

Fig. 14. (i) $H_v$ and (ii)$V_v$ SALS patterns of PBT/Epoxy blends crystallized at 125 °C for (a) PBT (b) 80/20 uncured blend (c) 80/20 cured blend.

Table 4
SAXS data for the PBT/epoxy uncured and cured blends

| Blend composition (PBT/epoxy) | Long period (Å) | Crystalline thickness (Å) | Amorphous thickness (Å) |
|---|---|---|---|
| 100/0[a] | 152 | 65.3 | 86.7 |
| 90/10 (uncured) | 194 | 87.3 | 106.7 |
| 80/20 (uncured) | 211 | 97.0 | 114.0 |
| 70/30 (uncured) | 258 | 149.6 | 132.0 |
| 60/40 (uncured) | Long period could not be calculated because of absence of clear diffraction maxima | | |
| 100/0[b] | 185 | 98.0 | 87.0 |
| 90/10 (cured) | 168 | 77.3 | 90.7 |
| 80/20 (cured)<br>70/30 (cured)<br>60/40 (cured) | Long period could not be calculated because of absence of clear diffraction maxima | | |

[a] Quenched from the melt state.

[b] Kept at curing temperature as for cured blends.

Table 5
Morphological parameters for PBT/epoxy uncured and cured blends crystallized at different temperature

| Crystallization temperature (°C) | Pure PBT | | | 80/20 (uncured) | | | 80/20 (cured) | | |
|---|---|---|---|---|---|---|---|---|---|
| | Nature of superstructure | Spherulitic radius (μm) | $I(V_v)/I(H_v)$ | Nature of superstructure | Spherulitic radius (μm) | $I(V_v)/I(H_v)$ | Nature of superstructure | Spherulitic radius (μm) | $I(V_v)/I(H_v)$ |
| 50 | Unusual | 3.2 | 1.0 | Usual | 4.0 | 1.2 | Usual | 3.9 | 1.8 |
| 75 | Unusual | 3.4 | 1.0 | Usual | 4.2 | 1.3 | Usual | 7.6 | 1.4 |
| 125 | Unusual | 4.0 | 1.03 | Mixed | 4.8 | 1.3 | Usual | 9.7 | 1.2 |
| 150 | Unusual | 4.2 | 1.07 | Mixed | 5.1 | 1.4 | Usual | 10.9 | 1.4 |
| 175 | Unusual | 6.2 | 1.1 | Mixed | 7.0 | 1.5 | Usual | 11.7 | 1.5 |
| 200 | Unusual | 7.0 | 1.1 | Unusual | 7.1 | 1.5 | Usual | 11.8 | 1.6 |
| 215 | Unusual | 7.1 | 1.1 | Unusual | 7.1 | 1.4 | Usual | 11.8 | 1.5 |

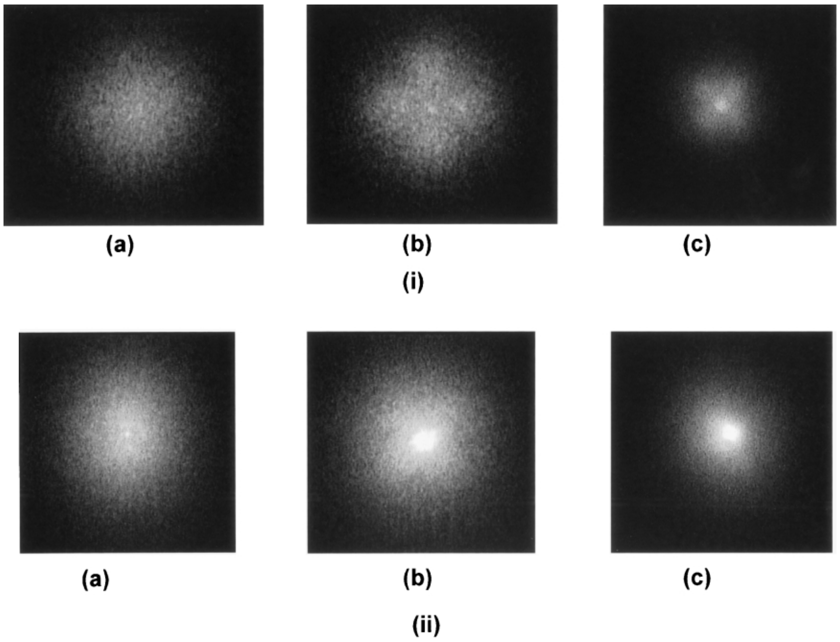

Fig. 15. (i) $H_v$ and (ii) $V_v$ SALS patterns of PBT/epoxy blends crystallized at 200 °C for (a) PBT (b) 80/20 uncured blend (c) 80/20 cured blend.

blending with a reactive solvent (epoxy) has been successfully carried out, with an aim of improving processing characteristics. Effect of uncured and cured epoxy resin on crystallization behavior and spherulitic morphology has been studied thus enhancing the understanding of thermoplastic-thermoset blend system. The salient observations of the above study are summarized below

1. In PBT/epoxy uncured blends, the half time of crystallization decreases while in the cured blends, half time of crystallization remains constant with increasing amount of epoxy resin.
2. The value of Avrami exponent varies between 1 and 2, indicating mixed type of spherulitic growth in pure PBT, PBT/epoxy uncured and cured blends at all temperatures.

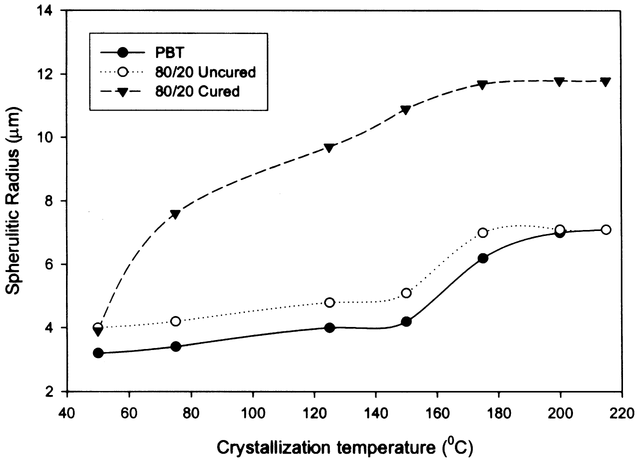

Fig. 16. Plot of spherulitic radius vs. crystallization temperature for PBT, PBT/epoxy 80/20 uncured and cured blends.

3. Four lobe unusual type $H_v$ pattern observed by SALS for isothermally crystallized PBT at 50 °C changed into four lobe usual type pattern in the presence of 20% or more epoxy resin in uncured and cured blends, thus showing that epoxy affects the growth of superstructure of PBT due to its miscibility.
4. Intensity of $V_v$ pattern is comparable to that of $H_v$ pattern in pure PBT isothermally crystallized at 50 °C, suggesting the formation of volume filled spherulitic structure. In the uncured as well as cured blends with 10% and greater amount of epoxy resin, $V_v$ intensity is high as compared to $H_v$ intensity, hence non-volume filled spherulites are formed in the blends. This is further confirmed by the optical micrographs.
5. Pure PBT shows four lobe unusual type of scattering pattern when crystallized isothermally at temperatures between 50 and 215 °C. PBT/epoxy 80/20 uncured blend, isothermally crystallized at temperatures between 50 and 150 °C shows usual type of pattern which changes into unusual type scattering pattern at 200 °C while PBT/epoxy 80/20 cured blend isothermally crystallized at temperatures between 50 and 215 °C shows only usual type of pattern. In pure PBT as well as in PBT/epoxy 80/20 uncured and cured blends, an increase in spherulitic radius is observed with increase in the crystallization temperature, as studied by SALS. The increase in the radius of spherulites levels off at 175 °C.

## References

[1] Venderbosch RW, Meijer HEH, Lemstra PJ. Polymer 1994;35:4349.
[2] Venderbosch RW, Meijer HEH, Lemstra PJ. Polymer 1995;36:1167.
[3] Venderbosch RW, Meijer HEH, Lemstra PJ. Polymer 1995;36:2903.

[4] Venderbosch RW. PhD Thesis, Eindhoven University of Technology, The Netherlands, 1995.

[5] Poncet S, Boiteux G, Pascault JP, Sautereau H, Seytre G, Rogozinski J, Kranbuehl D. Polymer 1999;40:6811.

[6] Ishii Y, Ryan AJ. Macromolecules 2000;33:158.

[7] Goosens JGP. PhD Thesis, Eindhoven University of Technology, The Netherlands, 1998.

[8] Saalbrink A, Mureau M, Peijs T. ICCH-Conference, Australia, 14–18 July, 1997.

[9] Jansen JP. PhD Thesis, Eindhoven University of Technology, The Netherlands, 1998.

[10] Ludwig HJ, Eyerer P. Polym Engng Sci 1988;28:143.

[11] Stein RS. In: Lenz RW, Stein RS, editors. Structure and properties of polymer films. New York: Plenum; 1973. p. 1–24.

[12] Stein RS, Misra A. J Polym Sci, Polym Phys Edn 1980;18:327.

[13] Roche EJ, Stein RS, Thomas EL. J Polym Sci Polym Phys Edn 1980; 18:1145.

[14] Garg SN, Misra A. J Polym Sci 1985;23:27.

[15] Misra A, Garg SN. J Polym Sci Part B: Polym Phys 1986;24:999.

[16] Misra A, Garg SN. J Polym Sci Part B: Polym Phys 1986;24:983.

[17] Halder RS, Joshi M, Misra A. J Appl Polym Sci 1990;39:1251.

[18] Dellimoy D, Bailley C, Devaux LA. Polym Engng Sci 1988;28(2): 104.

[19] Oyanguren PA, Frontini PM, Williams RJJ, Reydet EG, Pascault JP. Polymer 1996;37(14):3079.

[20] Oyanguren PA, Frontini PM, Williams RJJ, Vigier G, Pascault JP. Polymer 1996;37(14):3087.

[21] Avrami M. J Chem Phys 1940;8:2123.

[22] Lin CC. Polym Engng Sci 1983;23:113.

[23] Wunderlich B, Macromolecular physics, vol. 2. New York: Academic Press; 1976. p. 146.

[24] Kulshreshtha B, Ghosh AK, Misra A. J Macromol Sci-Phys 2002; in press.

[25] Kulshreshtha B. PhD Thesis, Indian Institute of Technology, Delhi, 2002.

[26] Stein RS, Cronauer J, Zachmann HG. J Mol Struct 1996;383:19.